Journal of Engineering and Sustainable Development
Vol. 23, No.06, November 2019
ISSN 2520-0917
https://doi.org/10.31272/jeasd.23.6.4

EFFECT OF NUMBER AND DISTRIBUTION OF SHEAR CONNECTORS ON THE COMPOSITE BOX-GIRDER BRIDGE UNDER ENVIRONMENTAL THERMAL CONDITIONS

*Dr. Hesham A. Numan[1], Ahmed Hussein Obed[2], Dr. Mustafa Özakça[3]

1) Lecturer Civil Engineering Department,Mustansiriyah University, Baghdad, Iraq.
2) Lecturer Civil Engineering Department, Mustansiriyah University, Baghdad, Iraq.
3) Prof., Civil Engineering Department, University of Gaziantep, Gaziantep, Turkey.

Received 15/5/2018 Accepted in revised form 9/10/2018 Published 1/11/2019

Abstract: This research deals with the thermal and thermo-structural behavior of concrete-steel composite box-girder bridge under the amalgamation of environmental thermal loads: global solar radiation, ambient air temperature, and wind speed. To achieve this goal, the experimental composite box-girder bridge segment with a full-scale cross-section erected in a campus of Gaziantep University, Turkey; and the series of numerical thermal analyses are conducted. The hourly fluctuations of the numerical temperatures matched well with the experimental ones. This research also submits a theoretical extensive study of the effect of shear connector's number and arrangement at the concrete-steel interface on the hourly vertical thermal movements with an emphasis on the degree of composite interaction. Under partial interaction, the hourly vertical thermal displacements findings are presented to more visualize the design life of such constructions, as well as, the economic aspects as regards to climatic impacts.

Keywords: *Composite Box-Girder Bridge, Environmental Thermal Loads, Temperature Fluctuations, Shear Connector's Number And Arrangement*.

تأثير عدد وتوزيع روابط القص على الجسر العارضة الصندوقي المركب تحت الظروف الحرارية البيئية

الخلاصة: يتناول هذا البحث التصرف الحراري والإنشائي-الحراري للكونكريت-حديد المركب لجسر العارضة الصندوقي تحت تأثير دمج الأحمال الحرارية البيئية: الإشعاع الشمسي الكلي ، درجة حرارة الهواء المحيط ، وسرعة الرياح. ولتحقيق هذا الهدف ، تم إنشاء جزء تجريبي لجسر العارضة الصندوقي المركب مع مقياس كامل للمقطع العرضي في حرم جامعة غازي عنتاب،تركيا ؛ وسلسلة من التحليلات الحرارية العددية أجريت. التقلبات بالساعات لدرجات الحرارة العددية متطابقة بشكل جيد مع تلك النتائج العملية. يقدم هذا البحث أيضًا دراسة نظرية مستفيضة عن تأثير عدد روابط القص وترتيبها عند السطح البيني الكونكريت-حديد على الحركات الحرارية العمودية بالساعات مع التركيز على درجة الترابط. تحت تأثير الترابط الجزئي، نتائج الازحات العمودية بالساعات قدمت لمزيد من التصور عن الحياة التصميمية لهكذا منشآت بالإضافة الى الناحية الاقتصادية قدر تعلق الأمر بالتأثيرات المناخية.

1. Introduction

Nowadays, composite box-girder bridges are extensively present in civil engineering projects due to its higher torsion stiffness, higher flexural capacity, rapid construction, economics, and long span capability. On the other hand, the closed form of a composite

**Corresponding Author* : dr.heshamnuman@uomustansiriyah.edu.iq

box girder makes the internal parts and boundaries of the steel girders a less vulnerable to corrosion from external factors. The composite action between the concrete slab and the steel girder is achieved by welding shear connectors on the top flanges of the steel girders.

Due to the bridge is constructed in an open environment; the bridge is constantly undergoing to exchange the heat energy with its surrounding environment. Therefore, the variation of temperature distributions within the bridge body is continually experiencing. Principally, the environmental thermal impacts comprise of global solar radiation, ambient air temperature, and wind speed, which altered at each time step of a day.

The issue of environmental thermal impacts on the performance of bridges during the design life became a required-study problem since Leonhardt et al. (1965) [1] founded the cracks in the Jagst Bridge in Germany as a result of the variation of temperature distribution along the depth of the superstructure bridge. The scholars reported that the width of the crack was 5 mm along one of the box webs. Capps (1968) [2] found that the change of ambient air temperature caused the large movement in a steel box bridge in England. Additionally, Fu et al. (1990) [3] pointed out that the minute cracks in the concrete deck of the composite bridges may be occurring due to climatic conditions. They indicated that these cracks may be subsequently grown result in existing service load on the bridge.

Depending on a comprehensive study conducted by Au et al. (2002) [4] about the thermal behavior of bridges in Hong Kong with confirmation on steel-concrete composite bridges. The findings of this study confirmed that the temperature distribution in bridge relies primarily on the solar radiation, atmospheric temperature, and wind speed in the vicinity. Other studies accomplished by (Grisham 2005, Writer 2007, and Chen et al. 2009) [5-7] pointed out that the thermal stresses may earnestly affect the design life of the bridges by causing cracks in the concrete slab or deflections and further deformations in the concrete component. Furthermore, the variation of temperature distributions under the certain environmental conditions was responsible for the evolution thermal stresses may be comparable to that induced by dead or live load emphasized by Xu et al. (2010) [8].

Based on field study was performed by Cao et al. (2011) [9] on the Zhanjiang Bay Bridge. The researchers observed that the maximum temperature gradient in the steel section was more than twice the design specification. Additionally, the behavior temperature curves along the cross-section of girder were a high degree of correlation with the instantaneous air temperatures depending on long-term temperature data accomplished by Ding et al. (2012) [10].

On the other hand, based on the Finite Element (FE) models and field vertical temperature readings during the daily thermal cycle; Quan (2008) [11] proposed the vertical temperature gradient for heating and cooling phases. The researcher compared between vertical temperature gradients for a certain return period (100-year) as suggested by AASHTO ones, and a good correlation found. Kim et al. (2009) [12] offered a simplified procedure to evaluate the three-dimensional (3D) temperature variation of curved steel box girder bridges by utilizing FE model based on a theoretical

solar radiation energy formula. They concluded that all the reaction forces of the curved bridges increased as the radius reduced and the span length increased. Besides, they detected that the chordal bearing setup exhibits larger reaction than the tangential bearing setup when the exterior web faces south direction. Furthermore, Xia et al. (2013) [13] performed FE simulation based on transient heat transfer analysis of a suspension bridge with a length of 2131-meter to investigate time-dependent temperature distributions for each component of the bridge. The numerical outcomes checked by comparison with field records at different times of day and in different seasons, and a good agreement achieved.

The main objective of the present study is to emulate the actual thermal performance demeanor of a composite box-girder bridge under full and partial composite interaction case. After an inclusive seeking, to the best of the authors' knowledge besides to the literature survey of this article, none of the formerly reviewed articles submitted the effects of composite interaction on the vertical thermal movements throughout the full range of time of a day. Additionally, both of the heat fluxes inside the enclosure system, and also the mutual irradiations between external bridge surfaces and the ambient air temperature simultaneously simulated. Besides to the transient heat conduction, surface convection, solar radiation, and reflected radiation modeled. All these concepts of heat transfer for such constructions are taken into account to fulfill a good agreement between experimental and numerical thermal results.

2. Mechanism of Heat Transfer in Composite Bridges

The heat conduction process within a composite box-girder bridge can be emulated through using 3D Fourier partial differential equation (Thaksin et al. 1977) [14]:

$$k\left(\frac{\partial^2 T}{\partial x^2}+\frac{\partial^2 T}{\partial y^2}+\frac{\partial^2 T}{\partial z^2}\right)=\rho c\frac{\partial T}{\partial t} \quad (1)$$

where k is the isotropic thermal conductivity coefficient of the material in Btu/hr/ft/˚F, T is the temperature at an arbitrary point (x, y, and z) in ˚F, ρ is the density of the material in Ib/ft^3, c is the specific heat of the material in Btu/Ib/˚F, and t is the time in hr. The thermal loads applied on the boundaries of the composite box-girder bridge, which associated with Eq. (1), can be expressed as follows:

$$k\left(\frac{\partial T}{\partial x}l_x+\frac{\partial T}{\partial y}l_y+\frac{\partial T}{\partial z}l_z\right)+q=0 \quad (2)$$

where l_x, l_y, and l_z are the direction cosines of the unit outwards vectors normal to the boundary surfaces of the bridge as defined by Ghali et al. (2002) [15], and q is the sum of all heat fluxes occurs on the exposed bridge surfaces in Btu/hr/ft^2, which can be represented as:

$$q=q_c+q_s+q_r+q_i \quad (3)$$

The term q_c represents the rate of convection heat transfer that happens between the exterior boundaries of the composite box-girder bridge and the surrounding air because

of the temperature difference between them. The heat convection q_c can be computed by using Newton's convection law (Thaksin et al. 1977) [14] as follows:

$$q_c = h_c(T_s - T_\infty) \quad (4)$$

where h_c is the convection coefficient between the surrounding air and the external composite girder surfaces in Btu/hr/ft^2/˚F, T_s is the external surface temperature of the composite bridge in ˚F, and T_∞ is the temperature of surrounding air in ˚F. In the present study, the following formula was originally recommended by Williamson (1967) [16] used to assess the convection coefficients h_c on all exterior surfaces of the composite girder:

$$h_c = 0.665 + 0.133\, w_s \quad (5)$$

where w_s is the wind speed in mph.

The term q_s refers to the incoming heat fluxes (short wave-radiation) from the sun on the external surfaces of the composite box-girder bridge (Lee 2010) [17]. This term can be determined through the following expression:

$$q_s = aI_s \quad (6)$$

where a is the absorption coefficient (absorptivity) of the external surface, and I_s is the global incoming solar radiation received by the exterior surfaces of the composite box-girder bridge in Btu/hr/ft^2.

q_r is the reflected solar radiation from the ground surface and from other objects surrounding the considered external boundary of the composite box-girder bridge. q_r depends on the reflective properties of the surfaces surrounding the considered external boundary and global radiation sticking the horizontal plane. However, q_r is defined as the ratio of the reflected radiation by a surface of the object to the global incident radiation on it, which is also defined as albedo.

$$q_r = aI_r \quad (7)$$

where I_r is the reflected radiation flux from the ground and the surroundings in Btu/hr/ft^2.

$$I_r = r_g I_s \frac{1-\cos\delta_1}{2} \quad (8)$$

where r_g is the reflection coefficient of the ground and from other objects surrounding the considered external boundary of the composite box-girder bridge (albedo). δ_1 is the inclination angle of the surfaces of bridge respect to the horizontal plane. The main assumption in this study was all surrounding surfaces have the same reflectivity and taken albedo equals to 0.25.

q_i is the net of the irradiation heat transfer occurred between the exposed bridge surfaces and ambient air can be expressed using Stefan-Boltzmann law:

$$q_i = \in S_t(T_s^4 - T_\infty^4) \quad (9)$$

where ∈ is the emissivity coefficient of the bridge surface, and S_t is the Stefan-Boltzman constant, which equals to 0.174×10^{-8} Btu/hr/ft^2/°R^4.

3. Experimental Work

Concrete-steel composite box-girder segment was erected on the campus of Gaziantep University, Turkey at Latitude 37° 02′ 22″ N and Longitude 37° 19′ 07″ E. The length of the experimental composite box-girder segment was 6.56 feet and with a single span. The location of the composite box-girder segment was selected fussily to be near enough from the laboratory buildings with a view to providing electric services along the experimental work. On the other hand, the location of the composite box-girder segment was away enough from surrounding objects (the buildings or structures) to avert the shading impacts. Figure 1 illustrates the components of the composite box-girder segment with details; where the upper component was concrete slab and the lower portion was the steel trapezoidal box girder.

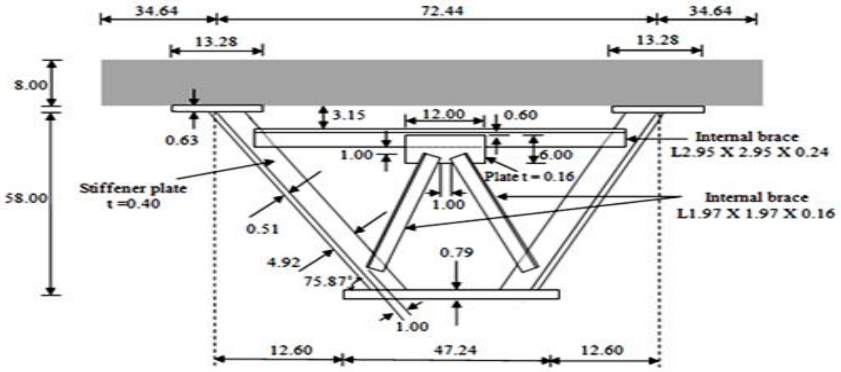

Figure 1 Cross-section of the experimental composite bridge segment (all dimensions in inches and not to scale)

To simulate the realistic ground reflected radiation and convection cooling; the superstructure of bridge segment lifted to a suitable height from the ground surface. The main difference in elevation between the lower surface of trapezoidal steel girder and the ground surface achieved through construction four reinforced columns with a height of 78.74 inches. Additionally, the thermal isolation along the cavity of the bridge implemented by sealing the faces of the cross-section of the superstructure of the bridge segment with the special insulation boards.

In the present work, the embedment and surface thermocouples type-T were used to measure temperatures of both the components. On the other hand, 108-temperature probe, CS300 pyranometer, and NRG#40 anemometer were used to measure ambient air temperature, global solar radiation and wind speed, respectively. Figure 2 shows the embedment and surface thermocouples, while Figure 3 shows the environmental sensors. All the devices belonged to the data acquisition system that used in this experimental work were provided by Campbell Scientific Inc. The data acquisition system was saved in two environmental enclosures to protect this system from the

external conditions (e.g., humidity, water, etc.). This system involved the CR1000 data logger, three AM16/32 multiplexers, the AVW200 spectrum analyzer, and the NL115 Ethernet/Compact Flash module. Two environmental enclosures placed inside the container, which is near from the experimental composite box-girder bridge, as shown in Figure 3. The experimental data collected at each one hour as a time step for a complete one-year cycle (from June 01, 2015 to May 31, 2016).

Figure 2 Thermocouple type-T (a) embedment (b) surface

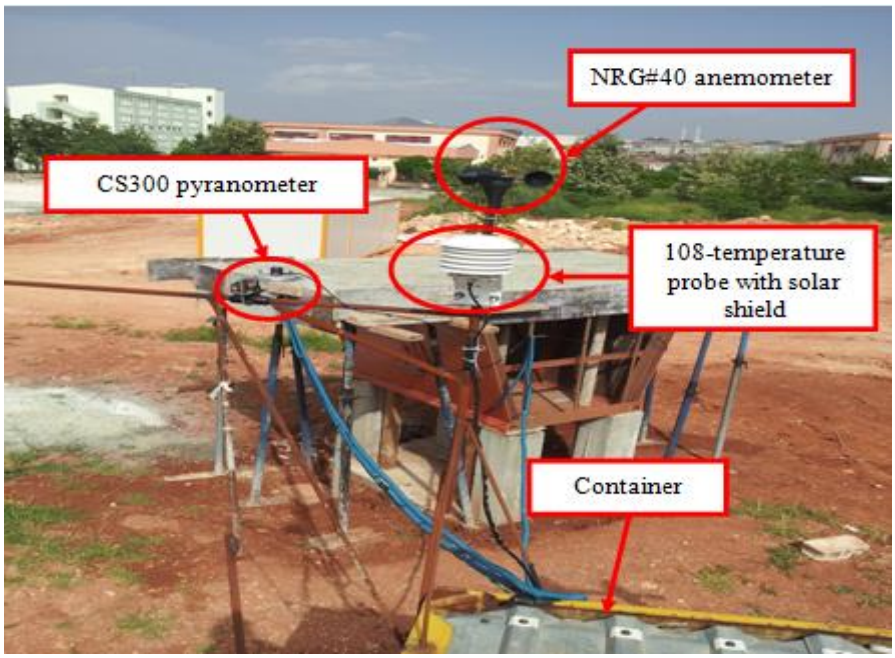

Figure 3 Environmental sensors used in the current study besides to the container

4. Distribution of the Thermocouples within the Composition System

As shown in Figure 4, thirty-two embedment and surface thermocouples were installed in the mid-span section of the experimental composite box-girder segment in addition to one thermocouple was hanged inside the box girder to measure the confined air temperature inside the enclosure system. The reason of distribution thermocouples at the mid-span was because the experimental composite box-girder segment is straight

and with uniform sections along its span; therefore the magnitude of sensitivity of the changing in the shape function of temperature distributions and gradients along the bridge's length is expected very small.

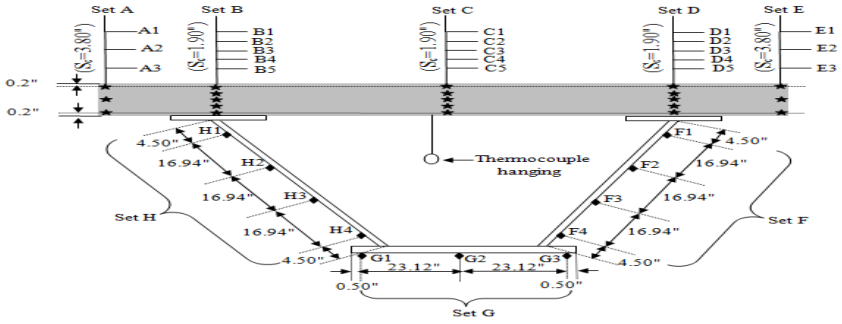

Figure 4 Thermocouples layout within the experimental composite box-girder bridge segment (all dimensions in inches)

5. Finite Element Thermal Analysis

To achieve the accuracy in the fluctuation of temperature distributions in a composition system at each time step of the daily environmental conditions, the hemi-cube method adopted through the commercial FE program COMSOL 4.3a (2012) [18] in the current study. This method simulates the shadowing effect on each element face at each time step of the solution depends on the sun trajectory during the daytime. From this consideration, the heat transfer with surface-to-surface radiation interface under the hemi-cube method was activated. However, the irradiative heat fluxes at the exposed surfaces of the composite box-girder (as a result of the mutual visions between them) under hemi-cube method modeled in COMSOL can be expressed by the following expression:

$$q_i = \in (G_i + F_\infty S_t T_s^4 - S_t T_\infty^4) \qquad (10)$$

where G_i is the reciprocal (mutual) irradiation arriving from other surfaces in Btu/hr/ft^2 (is a function of the radiosity at any other point in view), and F_∞ is the ambient view factor, i.e. prescribes the fraction of view from each point that is not covered by other boundaries.

Moreover, to highlight the total radiation heat fluxes that arise from inside the cavity of the composite box-girder segment, the radiation in participating media interface was also activated in the current analysis. Radiation participating media interface in COMSOL uses the discrete ordinate method. This method is discussed three meanings of the interaction process, which are: absorption, emission, and scattering at each surface inside the cavity, and it solves them simultaneously. The discrete ordinate method with a maximum resolution of 80 discrete angular directions (S8) was used to diagnose the total heat fluxes generated from the inside cavity of the composite box-girder segment, and to calculate incident radiation distributions. Hence, Eq. 3 was evolved by adding an extra term that is q_n to simulate the total radiation heat fluxes inside the enclosure system. On the other hand, the heat transfer with surface-to-surface

radiation and radiation participating media interfaces are merged with the solid mechanics module to form the thermal stress module in COMSOL package. The aim of forming the thermal stress module to predict the changing in temperature and thermo-structural response at any point within the model at each time step throughout a day.

Due to the vertical and horizontal temperature fluctuations in a bridge are generally close to uniform from about 4 a.m. to about just before sunrise time. Thus, both of the values of the initial bridge and strain reference temperatures are imposed equal to mean thermocouples value at 04:00 a.m. On the other hand, the combined environmental thermal loadings are inserted before three days from the intended day.

To simulate the realistic heat transfer in the composition system the thermal properties of each components were carefully selected to be within the possible range of thermal properties that suggested by (Somerton 1992, Duffie and Beckman 2006, Kothandaraman 2006, Mehta and Monteiro 2006, Incropera et al. 2007, and Wang et al. 2010) [19-24]. The values of thermal properties for two components were depicted in Table 1.

Table 1 Values of thermal properties

Material property	Concrete	Steel
Thermal Conductivity (Btu/hr/ft/˚F), k	0.81	26.6
Specific heat (Btu/lb/˚F), c	0.23	0.11
Absorptivity, a	0.50	0.65
Emissivity, $\in$	0.90	0.95
Density (lb/ft^3), ρ	150	490

Where the modulus of elasticity of the concrete slab and steel girder were 3.69×10^6 psi, 29.00×10^6 psi, respectively, while the Poisson's ratio of the concrete slab and steel girder were 0.2, and 0.3, respectively. It should be noted that the structural properties of the steel girder including yield stress and tensile strength were 4.99×10^4 psi and 5.99×10^4 psi, respectively.

6. Comparison of Experimental and Numerical Findings

In this study, the series of compressions have been done between the experimental and numerical temperatures to verify the current thermal FE model. These comparisons were along the full range of time of the perfect thermal days (sunny and clear days) from four seasons during the whole experimental period. The selected days were August 03, 2015, October 08, 2015, and January 13, 2016, March 24, 2016, to simulate summer, fall, winter, and spring conditions, respectively. The hourly meteorological measurements involving global incoming solar radiation, ambient air temperature, and wind speed for the selected days used as thermal load inputs of the current FE model. Figure 5 depicts the comparisons between the experimental and the numerical findings for the selected thermocouples. The selection thermocouples were C3, H3, and F3. In

these figures, EXP indicates to experimental results, while NUM indicates to the presented numerical 3D model findings.

Two statistical concepts are used to clarify the grade of convergence between the experimental and the numerical findings. The first concept was the Maximum Absolute Difference (MAD), and it refers to the maximum absolute difference between the experimental and the numerical findings at each thermocouple site during the tested day. The second one was the Average Absolute Difference (AAD) that is the summation of the absolute differences between the experimental and the numerical results at each thermocouple site divided by the total number of the time steps of the tested day. Smaller values of MAD and AAD signify that the grade of convergence between the experimental and the numerical results is excellent.

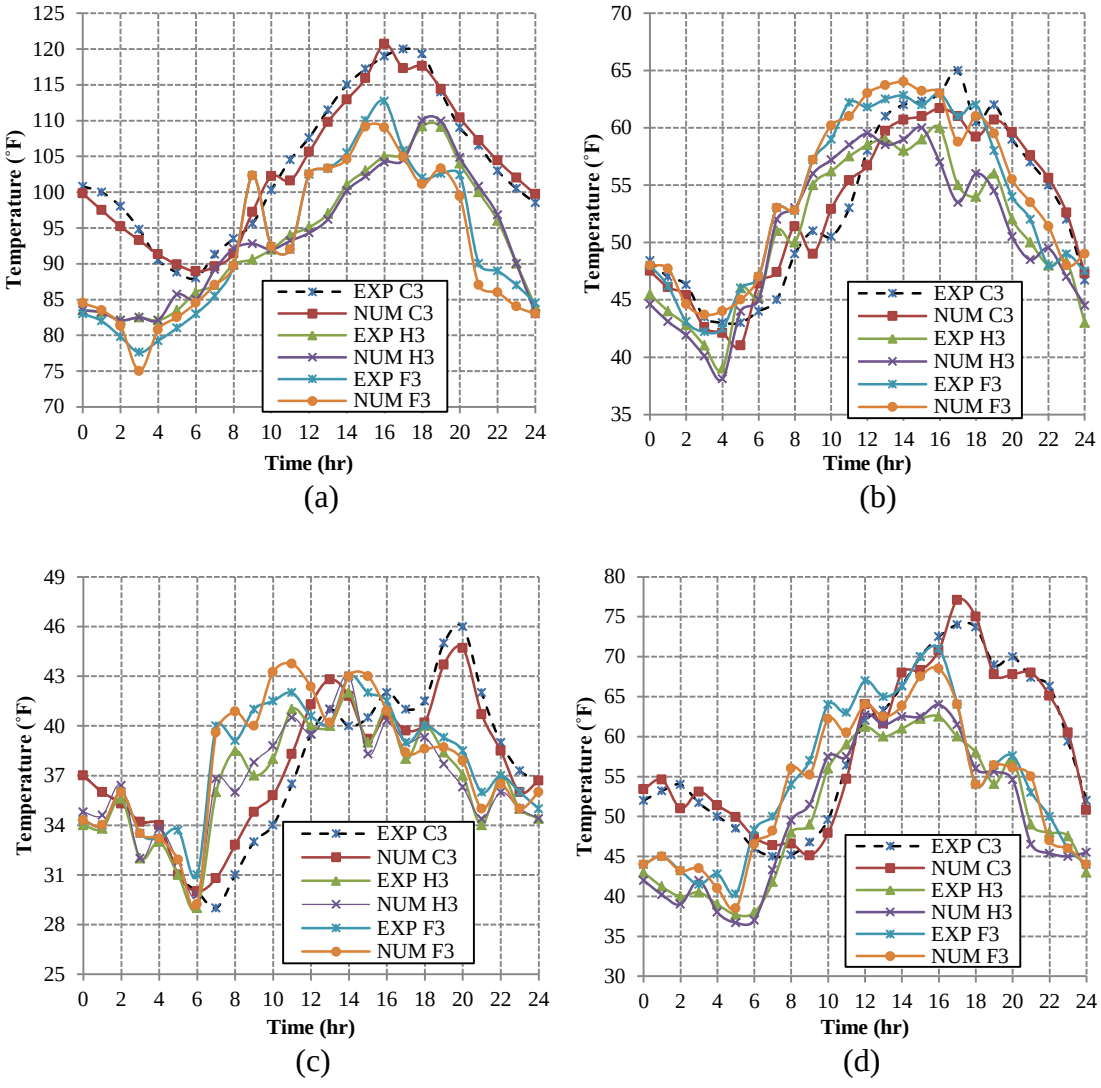

Figure 5 Comparison of experimental and numerical temperatures for selection thermocouples on: (a) August 03, 2015, (b) October 08, 2015, (c) on January 13, 2016, and (d) on March 24, 2016

As shown in Figure 5, a good harmony achieved between the shape of numerical and the experimental temperature functions during the full range of selected days. In this

study, the minimum and maximum values of MAD occurred on March 24. The minimum value of MAD took place at thermocouple B2 with a value of 1.03˚F, while the maximum value of MAD took place at thermocouple C1 with a value of 4.50 ˚F. On the other hand, the minimum and maximum values of AAD took place at thermocouple C5 with a value of 0.36 on January 13 and 2.06 on March 24, respectively. From the results of MAD and AAD, besides to the comparisons that illustrated in Figure 5, it can be said that the current FE could efficiently to simulate the thermal performance of the composite box-girder segment under the different conditions of environmental loadings.

7. Finite Element Model of Shear Connector

By using COMSOL v4.3 (2012) [18], the 3D FE simulation conducted with spanning the experimental composite box girder bride to 1200 inches (100 feet). To characterize the influences of both the number of studs and arrangement on the hourly results of vertical thermal movement (vertical thermal displacement) throughout the examined day, four parameters were held constant including: the orientation of the bridge at east-west direction, the geometrical configuration of the bridge, all mechanical and thermal characteristics of ingredients (concrete, steel, and stud shear connector) in the composite box- girder bridge, and dimension size of stud shear connector. A linear elastic material is assumed to the behavior of headed stud model with the modulus of elasticity and yield stress 2.90×10^6 psi and 6.82×10^4 psi, respectively, while the thermal properties of studs still as the steel girder. On the other hand, the other properties of the concrete and steel components remained the same as illustrated in Table 1.

The inputs of hourly thermal loads (global insolation, ambient air temperature, and wind speed) in the current analyses are based on the meteorological readings in the selected day, which also were August 03, 2015, October 08, 2015, January 13, 2016, and March 24, 2016.

By taking advantage of the rigid connector interface in solid mechanics module of the COMSOL software; the headed studs designated as rigid links to model a stiff constraint case happening between two bodies (concrete and steel). Six Degree Of Freedoms (DOFs) are taken into account in the solid geometry of headed stud with neglecting of the occurrence finite rotations in all of the headed studs. The dimensional geometry of the headed studs were modeled based on the used range of dimensional geometry of headed stud in practical design objective that offered by Johnson (1975) [25]. The total length of the headed stud was 3.93 inches and with a diameter equal to 0.75 inches.

In the present work, the full-degree composite interaction assumed is achieved through distributing a large number of rigid links respect to the proposed configuration of the box-girder bridge. The bridge's span was divided into 200 divisions and with a total number of rigid links by 1200. At the top surface of each flange of the steel box-girder, the shear studs distributed as rigid links in three rows along the span length of the bridge with an equal spacing of 5.97 inches (from center to center between two rows). In the longitudinal direction of the upper surface of the top flanges of the steel girder, the initial and ending distances in the first rows and last rows of shear studs were

equal and taken as 3.00 inches. These distances represent the spacing between the free edge and the center nearest row of shear studs.

On the other hand, in the transverse direction of each top flange of the steel girder, the space between connectors was 5.01 inches (center-to-center) and with a clear distance of 1.25 inches (between the edge and the nearest connector). In the current study, the distributions of shear studs in the longitudinal and transverse direction of each the top flange of the steel girder based on the limitations of spaces between the shear connectors of the composition system provided by (AASHTO LRFD 2012, and Narendra 2015) [26,27]. The mesh of superstructure with headed studs under full composite interaction, as shown in Figure 6.

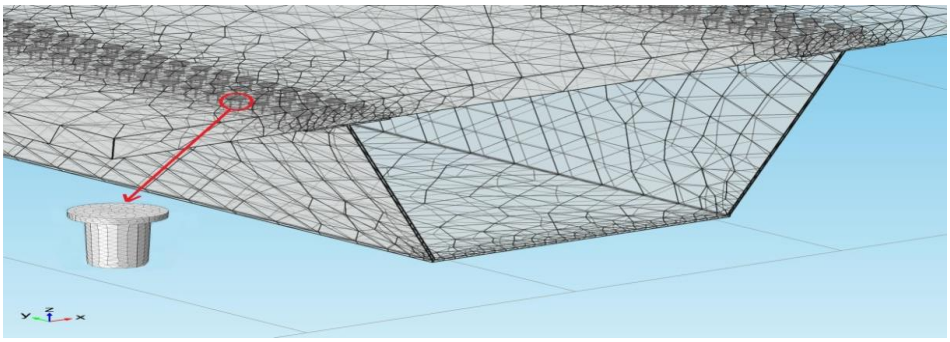

Figure 6 Mesh the composition system in full interaction

8. The Strategy of Changing the Number and Spacing of Shear Connectors

Since the degree of composite interaction (shear connection ratio) is defined as the ratio of the actual number of shear studs to the necessary number in fully jointed composite structures (Li et al. 2014) [28]. Therefore, the strategy of changing the total number of shear studs was by reducing the studs that provide the case of full composite interaction until approaching to the minimum degree of composite interaction case. For both solid and ribbed slabs and under U.S units, Eurocode 4 (CEN 1992) [29] stipulated that the minimum percentage of composite interaction by taking the smaller value of (0.40 or 0.25+0.01L*), where L* refers to the length of the composite member in the foot. Therefore, the minimum degree of composite interaction is considered 40% based on the proposed span length of the current composite box-girder model.

The present strategy of reduction of stud shear connectors based on removing the entire rows in the transverse axis of the composite bridge (x-direction) for each proposed stage of percentage reduction. The reason to select the procedure of reduction of shear connectors to be within x-direction of the composite bridge specifically is due to this direction is more influential on the vertical displacement results than the reduction of shear connectors in the y-direction (longitudinal axis of the bridge) (Muthanna 2015) [30]. It should be noted that the process of reduction achieved for all interior rows of stud shear connectors along the bridge length with excluding both of the first and last rows of the removal.

In the present work, the reduction of the total number of stud shear connectors from the interconnection zone between the concrete slab and steel girder done with a uniform step of 20% from the total number of stud shear connectors that give the complete composite interaction case (100%). Therefore, the percentages of the total number of stud shear connectors to the total number at the complete composite interaction were 80%, 60%, and 40%, respectively. The total number of stud shear connectors was 960, 720, and 480 when the composite interaction decreased from 100% to 80%, 60%, and 40%, respectively.

The percentage of composite interaction at 80%, 60%, and 40% degree touted as a partial interaction between the components, but there is an important note must be taken into consideration that the computation of slip ignored in this study.

After each reduction step, the spacing (S_r) between the rows of stud shear connectors in the longitudinal direction of the bridge (center-to-center) was gradually increased from 5.97 to 14.93 inches when the percentage of composite interaction changed from 100% to 40%. For each percentage of reduction proposed, the re-distribution in the transverse rows of stud shear connectors occurred and assumed the spacing (S_r) between them equally. In this study, the used spacing (S_r) in any percentage reduction of stud shear connectors was still compatible with the possible range of shear connector spacing to that recommended by (AASHTO LRFD 2012, and Narendra 2015) [26, 27].

To more conceive about the procedure in the computation spacing (S_r) for each percentage of reduction of the composite interaction, the simplest equation used as shown below:

$$S_r = \frac{L-D}{P_r \times N_d} \qquad (11)$$

where *L* refers to the total length of the composite box-girder bridge in inch, *D* is the sum of the clear distances between the first and last rows of stud shear connectors and adjacent free edge for each of them in inch, P_r is the percentage of reduction, and N_d is the number of divisions along the bridge's span.

9. Findings for Stud Connectors Reduction

Figure 7 illustrates the downward and upward vertical thermal displacements during the full range of time of the summer's day (August 03, 2015). The maximum downward thermal displacement recorded during the late dark hours (at 05:00 a.m.) in the degree of composite interaction of 80% and was about 0.21 inches. The maximum downward thermal displacement was decreased by about 26.83% when of the degree of composite interaction reduced from 80% to 40%. On the other hand, the maximum upward thermal displacement recorded during the daylight hours at around 02:00 p.m. with a value of approximately 0.47 inches at 80% degree of the composite interaction too. It can be also noticed that the maximum value of upward thermal displacement decreased by approximately 10.75% when the degree of composite interaction decreased from 80% to 40%.

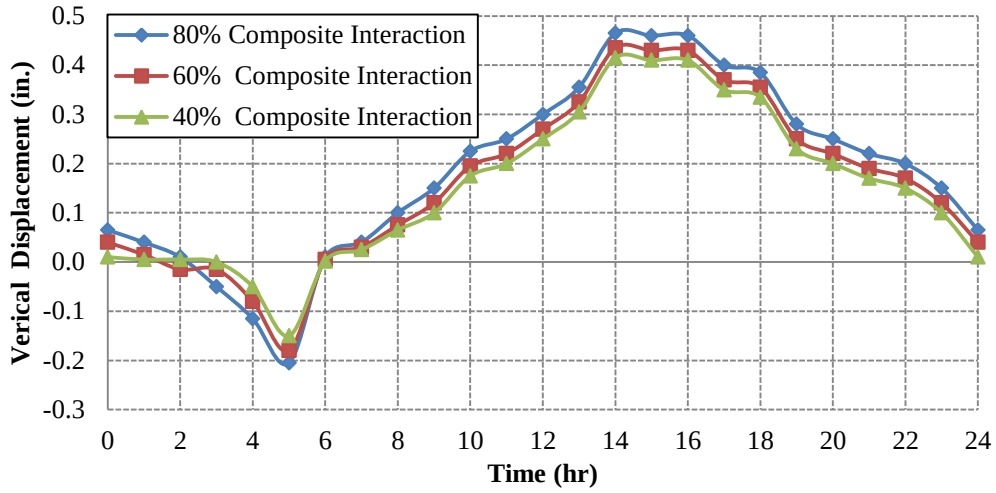

Figure 7 Hourly vertical thermal displacements against the reduction composite interaction during August 03, 2015

On October 08, 2015, Figure 8 depicts the distributions of vertical thermal displacements under the proposed degrees of composite interaction. As shown in this figure, the maximum downward thermal displacement decreased by about 15.62% and 28.13% resulted from a decrease the degree of the composite interaction from 80% to 60%, and 40%, respectively. On the other hand, the maximum upward thermal displacement decreased by about 6.25% and 15.00% when the degree of the composite interaction decreased from 80% to 60%, and 40%, respectively. However, during the 24 hours of the fall's day, the maximum absolute vertical thermal displacements for three degrees of composite interaction recorded at about 01:00 p.m., as illustrated in Figure 8.

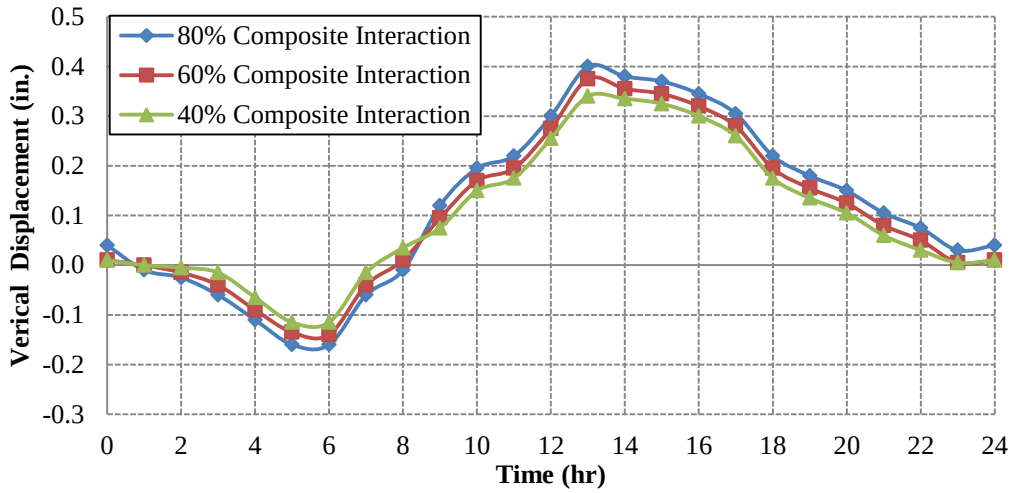

Figure 8 Hourly vertical thermal displacements against the reduction composite interaction during October 08, 2015

As shown in Figure 9, the absolute maximum value of the vertical thermal displacement was 0.25 inches, which occurred at the degree of composite interaction of 80% at the time step 12:00 p.m. during the selected winter conditions (January 13, 2016). The outcomes graphed in Figure 8.9 indicate that the maximum downward thermal displacement dropped by approximately 6.89% and 27.60% when the stud shear connectors reduced from 80% to 60%, and 40%, respectively. At the same time, the reduction of stud shear connectors from 80% to 60%, and 40%, respectively, it was accompanied by decreases in the upward thermal displacement by about 8% and 18%.

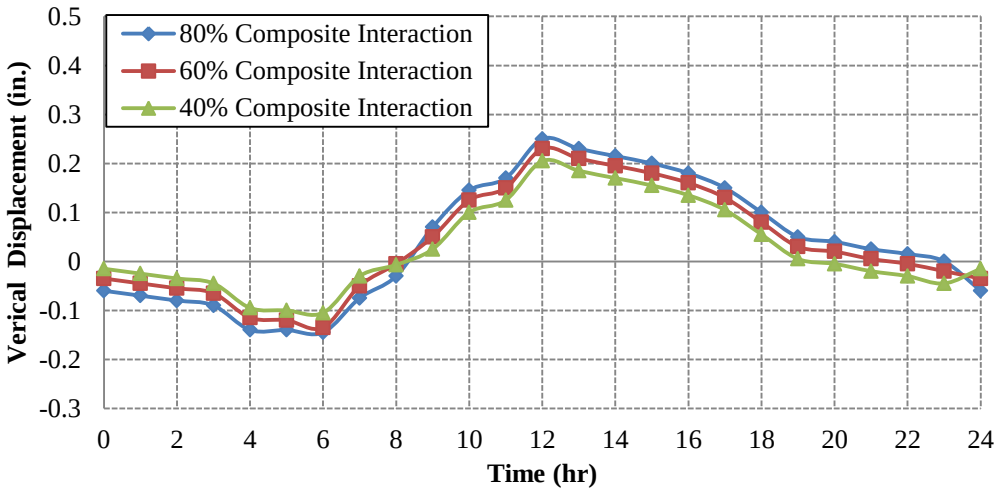

Figure 9 Hourly vertical thermal displacements against the reduction composite interaction during January 13, 2016

Figure 10 illustrates the effect of the degree of the composite interaction on the vertical thermal displacements during the spring day (March 24, 2016). From this figure, it is clearly can be noted that both the highest downward and upward thermal displacements recorded on the degree of the composite interaction of 80% were approximately 0.18 inches and 0.43 inches, respectively. As a result of decreasing the degree of composite interaction from 80% to 60%, and 40%, the downward thermal displacement was decreased by approximately 19.50% and 33.34%, and the decrease the upward thermal displacement of approximately 4.71%, and 8.24%. However, the results plotted in Figure 8.10 indicate that the absolute maximum vertical thermal displacements occurred at the time step 01:30 p.m. at different degrees of the composite interaction.

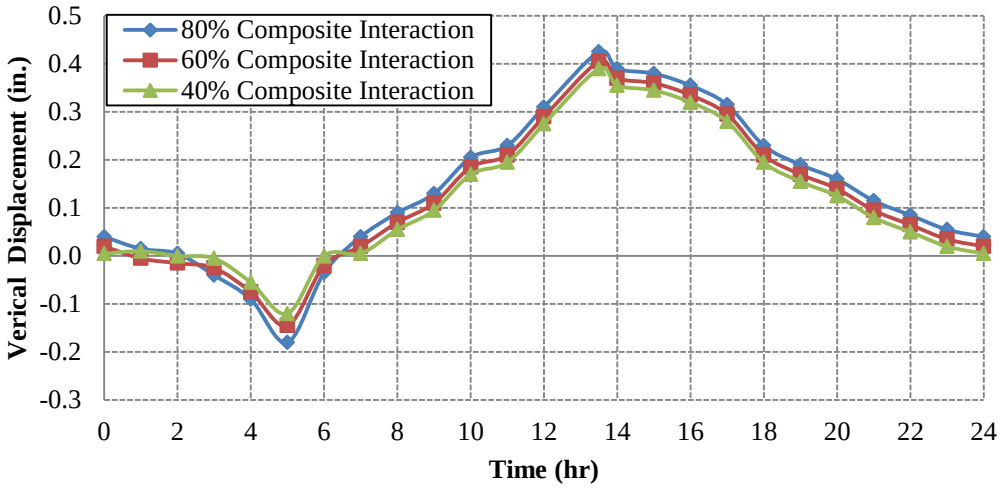

Figure 10 Hourly vertical thermal displacements against the reduction composite interaction during March 24, 2016

The outcomes graphed from Figures 7 to 10 occurred because the studs made of steel and the steel material is as well known as a relatively high thermal conductivity, therefore the decrease of composite interaction degree accompanied by loss good thermal conductors within the composition system. Thereby, the rate of heat flow between two components of the composition system by conduction reduced when decreasing the number of studs, and hence, reducing the amount of the thermal energy stored in the composite structures.

Another important note on these figures that is the time of the day at which the vertical thermal displacement reaches a maximum absolute value varies for all selected days. This is because of the differences of the sunrise and sunset times and the length of the daytime for these days. Additionally, the behavior of distribution of the vertical thermal displacements during the full range of the chosen days versus the proposed degree of composite interaction was similar by and large.

At 80% degree of composite interaction, Figures 11 to 14 illustrate the 3D views the mode shapes of vertical thermal displacements of the FE modeled composite box-girder when the maximum downward and upward displacements recorded in the mid-span and width of the bottom outer surface of the steel girder during the selected four days.

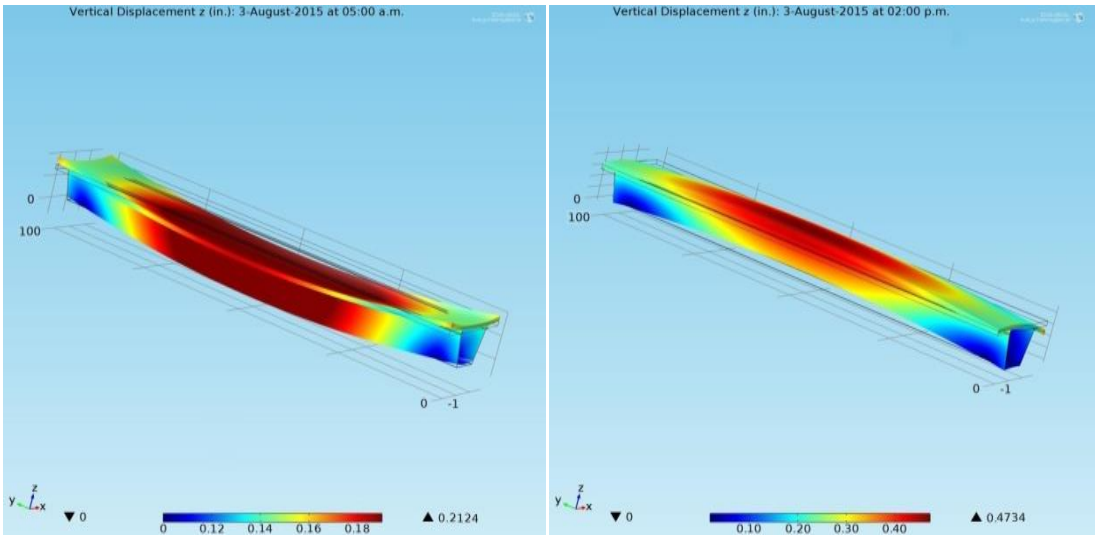

(a) (b)

Figure 11 3D views of the vertical thermal displacements on August 03, 2015:
(a) Maximum downward thermal displacement at 05:00 a.m.
(b) Maximum upward thermal displacement at 02:00 p.m.

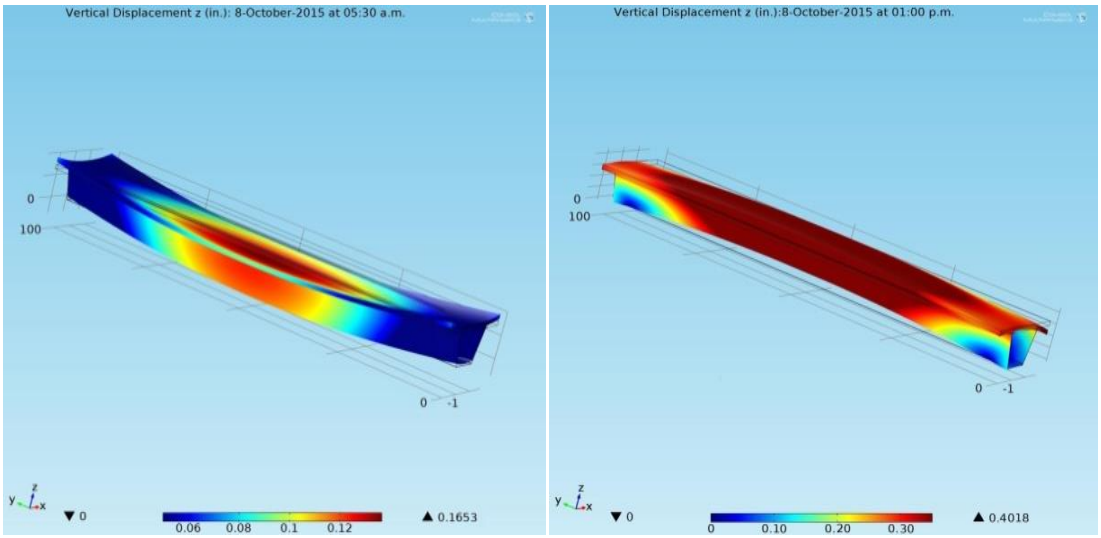

(a) (b)

Figure 12 3D views of the vertical thermal displacements on October 08, 2015:
(a) Maximum downward thermal displacement at 05:30 a.m.
(b) Maximum upward thermal displacement at 01:00 p.m.

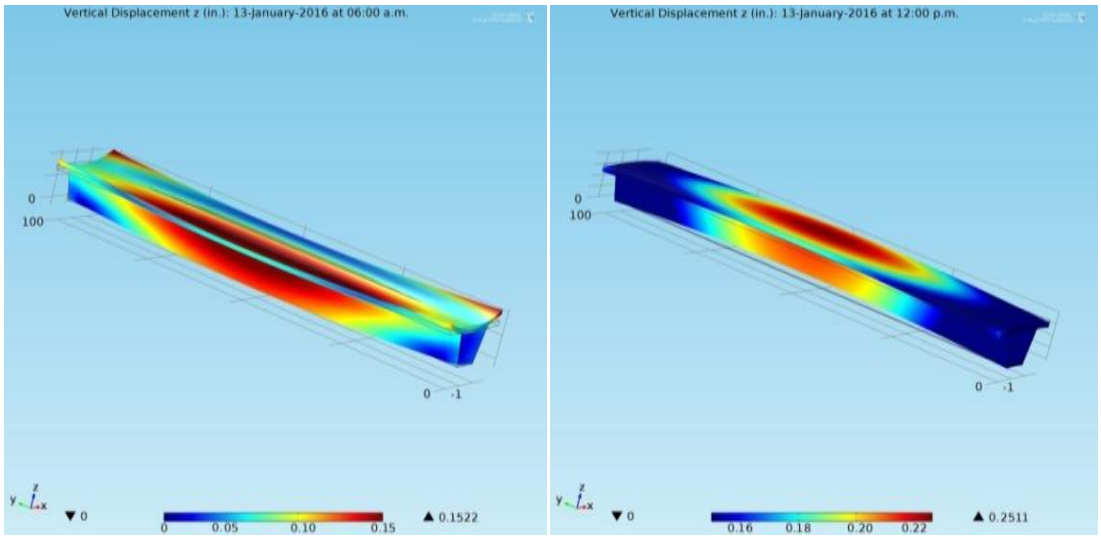

(a) (b)

Figure 13 3D views of the vertical thermal displacements on January 13, 2016:
(a) Maximum downward thermal displacement at 06:00 a.m.
(b) Maximum upward thermal displacement at 12:00 p.m.

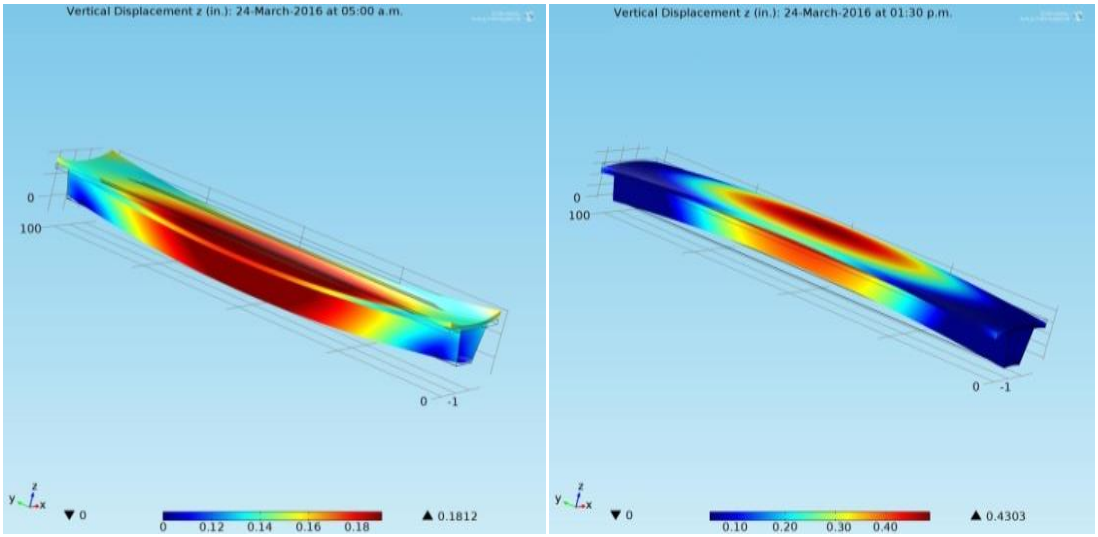

(a) (b)

Figure 14 3D views of the vertical thermal displacements on March 24, 2016:
(a) Maximum downward thermal displacement at 05:00 a.m.
(b) Maximum upward thermal displacement at 01:30 p.m.

10. Conclusions

In this paper, the experimental composite box-girder bridge segment and numerical thermal analyses were used to provide more visibility on the thermal and thermo-structural behavior of such constructions. The main conclusions of this study drawn as follows:

1. The range of MAD from 1.03 to 4.50˚F, while the values of the AAD ranged from 0.36 to 2.06˚F. Therefore, the present FE model in this study could efficiently emulate the actual alteration of temperature distributions in the

experimental composite box-girder segment with varying weather conditions. Subsequently, the current model gives more insight into the thermal behavior of any composite steel girder systems.

2. At one exemplary day taken from each season, the largest absolute value of the downward and upward thermal displacements recorded during the summer's day. When decreasing the degree of composite interaction from 80% to 40%, the maximum downward thermal displacement was decreased by approximately 26.83%, 28.13%, 27.59%, and 33.34% under the summer, fall, winter, and spring days, respectively. Similarly, the decrease from the degree of composite interaction from 80% to 40%, the maximum value of the upward thermal displacement corresponding days were decreased by about 10.75%, 15.00%, 18.00%, and 8.24%, respectively.
3. Under different daily thermal conditions, the trend of distribution of the vertical thermal displacements versus the time steps for all proposed degree of composite interaction was similar by and large.
4. A closer look at the calculated hourly findings of the vertical thermal displacements illustrates that the full composite interaction was achieved in COMSOL with minimum rigid connectors along the steel-concrete interface respect to the environmental thermal loadings. In other words, the behavior of composite portions was still as they before reduction that means the full interaction between components kept.
5. The simple procedure of changing the shear connector's number and redistribution again presented in this study gives us an opportunity to visualize the vertical thermal movement at each time step without resorting to the experimental thermal tests that are always costly. Another an important issue must be taken into consideration that no-interaction case between the concrete slab and the steel girder was not studied.
6. The increase of rigid shear connectors has an adverse effect on the stability of a composite box-girder during different environmental thermal conditions. Therefore, as regards to the economic feasibility of erecting such structures; the reduction of rigid shear connectors within the possible range of design codes is considered the best choice in order to the extent of the design life of the composite box-girder bridge against the climatic impacts.
7. The rigid link used in this study proves the ability to simulate the complicated thermal behavior of the composite box-girder bridge, and it can be utilized as a practical modeling technique for the long span of such construction.
8. The current study provides the opportunity to develop insights into future works such as emulation the influences of the composite continuous box-girder bridge, curved bridge, and changing the thermal material properties for each component on the thermal behaviors for such constructions.

11. References

1. Leonhardt, F., Kolbe, G., Peter, J. (1965). *Temperature differences endanger tension concrete bridge.* Concrete and Reinforced Concrete Construction, Vol. 60, No. 7, pp. 157-163.
2. Capps, M. W. R. (1968). *"The thermal behavior of the beachley viaduct/wye bridge"*. RRL Report, LR 234, Road Research Laboratory, Ministry of Transport, London, England.
3. Fu, H. C., Ng, S. F., Cheung, M. S. (1990). *Thermal behavior of composite bridges.* Journal of Structural Engineering, Vol. 116, No. 12, pp. 3302-3323.
4. Au, F. T. K, Cheung, S. K., Tham, L. G. (2002). *Design thermal loading for composite bridges in tropical region.* Steel and Composite Structures, Vol. 2, No. 6, pp. 441-460.
5. Grisham, G. P. (2005). *"Field Measurements of Bearing Displacements in Steel Girder Bridges"*. M.Sc. Thesis, University of Houston, USA.
6. Writer E. T. (2007). *"Field Study of Thermal Effects in Steel Plate and Box Girder Bridges"*. M.Sc. Thesis, University of Houston, USA.
7. Chen, B., Ding, R., Zheng, J., Zhang, S. (2009). *Field test on temperature field and thermal stress for prestressed concrete box-girder bridge.* Frontier of Architecture and Civil Engineering in China, Vol. 3, No. 2, pp. 158-164.
8. Xu, Y. L., Chen, B., Ng, C.L., Wong, K. Y, Chan, W.Y. (2010). *Monitoring temperature effect on a long suspension bridge.* Structural Control and Health monitoring, Vol. 17, No. 6, pp. 632-653.
9. Cao, Y., Yim, J., Zhao, Y., Wang, M. L. (2011). *Temperature effects on cable stayed bridge using health monitoring system: a case study*. Structural Health monitoring, Vol. 10, No. 5, pp. 523-537.
10. Ding, Y., Zhou, G., Li, A., Wang, G. (2012). *Thermal field characteristic analysis of steel box girder based on long-term measurement data.* International Journal of Steel Structures, Vol. 12, No. 2, pp. 219-232.
11. Quan, C. (2008). *"Effects of Thermal loads on Texas Steel Bridges"*. Ph.D. Thesis, University of Texas at Austin, Texas, USA.
12. Kim, S.-H., Cho, K.-I., Won, J.-H., Kim, J.-H. (2009). *A study on thermal behavior of curved steel box girder bridges considering solar radiation*. Archives of Civil and Mechanical Engineering, Vol. 9, No. 3, pp. 59-76.
13. Xia, Y., Chen, B., Zhou, X.-Q., Xu, Y.-L. (2013). *Field monitoring and numerical analysis of Tsing Ma suspension bridge temperature behavior*. Structural Control Health Monitoring, Vol. 20, No. 4, pp. 560-575.
14. Thaksin, T., Johnson, C. P., Matlock, H. (1977). *"Prediction of temperature and stresses in highway bridges by a numerical procedure using daily weather reports"*. Report FHWATX-77-23-l, Center for Highway Research, University of Texas at Austin, USA.
15. Ghali, A., Favre, R., Elbadry, M. (2002). *"Concrete structures: stresses and deformation "*. 3rd ed., London: E and FN Spon.

16. Williamson, P. J. (1967). *"The estimation of heat outputs for road heating installations"*. Road Research Laboratory, LR Report 77, Ministry of Transport, London, UK.
17. Lee, J. H. (2010). *"Experimental and Analytical Investigations of the Thermal Behavior of Prestressed Concrete Bridge Girders Including Imperfections"*. Ph.D. Thesis, Georgia Institute of Technology, Atlanta, USA.
18. COMSOL Multiphysics v4.3a. (2012). *"COMSOL Multiphysics user's guide"*, Stockhom, Sweden.
19. Somerton, W. H. (1992). *"Thermal properties and temperature-related behavior of rock/fluid systems"*. Vol. 37: 1st ed., Amsterdam, Netherlands: Elsevier Science.
20. Duffie, J. A., Beckman, W. A. (2006). *"Solar engineering of thermal processes"*. 3rd ed., New Jersey, USA: John Wiley and Son Inc.
21. Kothandaraman, C. P. (2006). *"Fundamental of heat and mass transfer"*. 3rd ed., New Delhi, India: New Age International.
22. Mehta, P. K., Monteiro, P. J. (2006). *"Concrete microstructure, properties, and materials"*. Vol. 3, New York: McGraw-Hill.
23. Incropera, F. P., Dewitt, D. P., Berrgman, T. L., Lavine, A. S. (2007). *"Fundamental of heat and mass transfer"*. 6th ed., New York, USA: John Willey and Sons Inc.
24. Wang, B., Wang, W., Zeng, X. (2010). *Measurements and analysis of temperature effects on box girders of continuous rigid frame bridges*. International Journal of Civil and Environmental Engineering, Vol. 4, No. 10, pp. 331-337.
25. Johnson, RP. (1975). *"Composite structures of steel and concrete, beams, columns, frames and applications in building"*. Vol.1, London: Crosby-Lockwood Staples.
26. AASHTO. (2012). *"AASHTO LRFD Bridge Design Specifications"*. Washington, D. C.
27. Narendra, T. (2015). *"Highway bridge superstructure enginering: LRFD approaches to design and analysis"*. Florida, USA: Taylor and Francis Group.
28. Li, Y-S., Li, S., Zhang, Y-L., Wang, J. Q. (2014). *"Experimental Research and Parameter Analysis on the Dynamic Factor of Railway Steel-Concrete Composite Beams"*. Proc. 9th Int. Conf. on Structural Dynamic, Eurodyn, Porto, Portugal, pp.1195-1201.
29. Eurocode 4. (1992). *"Design of composite steel and concrete structures"*. CEN, Part 1-1: General rules and rules for buildings. Brussels, Belgium.
30. Muthanna, A. N. (2015). *"Modelling and Analysis of Interface in Composite Box Girder Bridges"*. Ph.D. Thesis, University of Gaziantep, Gaziantep, Turkey.